NeuroImage: Clinical 21 (2019) 101600

Contents lists available at ScienceDirect

NeuroImage: Clinical

journal homepage: www.elsevier.com/locate/ynicl

Large-scale brain functional network topology disruptions underlie symptom heterogeneity in children with attention-deficit/hyperactivity disorder

Xing Qian[a], Francisco Xavier Castellanos[d], Lucina Q. Uddin[e], Beatrice Rui Yi Loo[a], Siwei Liu[a], Hui Li Koh[a], Xue Wei Wendy Poh[b], Daniel Fung[b], Cuntai Guan[f], Tih-Shih Lee[a], Choon Guan Lim[b,1], Juan Zhou[a,c,*,1]

[a] Center for Cognitive Neuroscience, Neuroscience & Behavioral Disorders Program, Duke-National University of Singapore Medical School, 8 College Road, Singapore 169857, Singapore
[b] Department of Child and Adolescent Psychiatry, Institute of Mental Health, Singapore, Singapore
[c] Clinical Imaging Research Centre, The Agency for Science, Technology and Research-National University of Singapore, Singapore, Singapore
[d] NYU Child Study Center, NYU Langone Medical Center, New York, NY, United States
[e] Department of Psychology, University of Miami, Coral Gables, FL, United States
[f] School of Computer Science and Engineering, Nanyang Technological University, Singapore, Singapore

ARTICLE INFO

Keywords:
Attention-deficit/hyperactivity disorder
Functional connectivity
Modularity
Heterogeneity

ABSTRACT

Accumulating evidence suggests brain network dysfunction in attention-deficit/hyperactivity disorder (ADHD). Whether large-scale brain network connectivity patterns reflect clinical heterogeneity in ADHD remains to be fully understood. This study aimed to characterize the differential within- and between-network functional connectivity (FC) changes in children with ADHD combined (ADHD-C) or inattentive (ADHD-I) subtypes and their associations with ADHD symptoms. We studied the task-free functional magnetic resonance imaging (fMRI) data of 58 boys with ADHD and 28 demographically matched healthy controls. We measured within- and between-network connectivity of both low-level (sensorimotor) and high-level (cognitive) large-scale intrinsic connectivity networks and network modularity. We found that children with ADHD-C but not those with ADHD-I exhibited hyper-connectivity within the anterior default mode network (DMN) compared with controls. Additionally, children with ADHD-C had higher inter-network FC between the left executive control (ECN) and the salience (SN) networks, between subcortical and visual networks, and between the DMN and left auditory networks than controls, while children with ADHD-I did not show differences compared with controls. Similarly, children with ADHD-C but not ADHD-I showed lower network modularity compared with controls. Importantly, these observed abnormal inter-network connectivity and network modularity metrics were associated with Child Behavioral Checklist (CBCL) attention-deficit/hyperactivity problems and internalizing problems in children with ADHD. This study revealed relatively greater loss of brain functional network segregation in childhood ADHD combined subtype compared to the inattentive subtype, suggesting differential large-scale functional brain network topology phenotype underlying childhood ADHD heterogeneity.

1. Introduction

Attention deficit/hyperactivity disorder (ADHD) is one of the most commonly diagnosed neuropsychiatric disorders of childhood. An individual affected by ADHD typically exhibits abnormal behaviors of inattention, hyperactivity and impulsivity, and these symptoms may persist into adulthood (Seymour & Miller, 2017; Kessler et al., 2005). ADHD is clinically heterogeneous and was categorized into three subtypes in the Diagnostic and Statistical Manual of Mental Disorders (DSM-IV): combined hyperactive-impulsive and inattentive subtype, predominantly inattentive subtype, and predominantly hyperactive-impulsive (relatively infrequent) subtype (Haack et al., 2017; Sahakian et al., 2015). As is the case with most mental disorders, the etiological bases and neural substrates of childhood ADHD are far from being fully

* Corresponding author.
E-mail address: helen.zhou@duke-nus.edu.sg (J. Zhou).
[1] Joint senior authors.

https://doi.org/10.1016/j.nicl.2018.11.010
Received 16 May 2018; Received in revised form 13 November 2018; Accepted 16 November 2018
Available online 19 November 2018

understood, especially the neurobiological basis underlying heterogeneity in childhood ADHD (dos Santos et al., 2014; Sharma & Couture, 2014).

Non-invasive neuroimaging methods open new avenues to characterize developmental changes in the human brain that engender complex cognitive abilities and the vulnerability patterns in neurodevelopmental disorders (Power et al., 2010; Menon, 2013; Khundrakpam et al., 2017). Intrinsic connectivity networks derived from resting-state functional magnetic resonance imaging (fMRI) index correlated low-frequency blood-oxygenation-level-dependent signal fluctuations between brain regions under resting or task-free conditions (Fox & Raichle, 2007; Biswal et al., 1995; Khundrakpam et al., 2016). Previous intrinsic connectivity network studies demonstrate that the human brain is functionally organized into large-scale connectivity networks with a hierarchical, modular structure (Meunier et al., 2009). This architecture allows for specialized processing to occur within densely interconnected groups of brain regions, which reduces interference among neural systems and facilitates cognitive performance (Bertolero et al., 2015). In the normal developing brain, the connections within or between these networks or modules exhibit characteristic patterns of maturation (Power et al., 2010). Studies using multiple methods reveal significant functional reconfigure of intrinsic connectivity networks with typical development: within-module connectivity increases while between-module connectivity declines, and this modular segregation serves as a substrate for the improvement of executive function capabilities (Cao et al., 2014a; Betzel et al., 2014; Baum et al., 2017). Abnormalities in brain network maturation play a significant role in ADHD (dos Santos et al., 2014; Fair et al., 2009).

Previous intrinsic connectivity network studies in childhood ADHD revealed abnormal functional connectivity (FC) in the default mode, executive control, salience and attention-related networks (Sidlauskaite et al., 2016; Bos et al., 2017), which were associated with ADHD-related symptoms such as distractibility and impaired executive function processing (Zhao et al., 2017; Francx et al., 2015). Nevertheless, these studies were often restricted to within-network FC of one or more specific brain circuits and it is relatively hard to compare across studies given differences in the location and shape of regions-of-interest (ROIs) for connectivity derivation. Comprehensive characterization of the whole-brain functional connectome, both within and between networks, is lacking in childhood ADHD. More importantly, as ADHD is a clinically heterogeneous condition, whether and how the ADHD subtypes may originate from different network breakdown mechanisms remains largely unknown. Several studies have begun to give some clues on the distinction of brain abnormalities of ADHD subtypes. Sanefuji and colleagues found that the hyperactive-impulsive subtype was associated with increased connectivity in the cortico-striatal network, whereas the inattentive subtype was associated with increased connectivity in the right ventral attention network (Sanefuji et al., 2017). Despite overlapping connectivity changes (particularly in the sensorimotor systems), the ADHD-C and ADHD-I subtypes demonstrated unique patterns of atypical connectivity (Fair et al., 2013). Moreover, other studies have indicated distinction of the activation regions during task performance, neuroanatomical organization, and microstructural changes across different ADHD subtypes (Saad et al., 2017; Lei et al., 2014; Shang et al., 2017). Nevertheless, a comprehensive understanding of large-scale intrinsic connectivity network modular topology underlying the clinical heterogeneity of ADHD is needed.

To address these gaps, we sought to compare the whole-brain large-scale functional network topology derived from task-free fMRI between children with ADHD subtypes and age and gender-matched healthy controls. Specifically, we elucidated alterations of both intra- and inter-network functional connectivity and modular network topology in ADHD inattentive (ADHD-I) and combined (ADHD-C) subtypes using independent component analysis (ICA) and graph theoretical approaches. Given previous findings suggesting a developmental lag of whole-brain functional networks in ADHD children (Sripada et al., 2014; Cao et al., 2014b), we hypothesized that ADHD would have loss of functional segregation between networks, corresponding to lower network modularity. Such network connectivity disruptions might differ between the two subtypes, and may relate to ADHD-specific symptom severity.

2. Methods

2.1. Participants

In total, 35 boys with ADHD-C and 23 boys with ADHD-I with ages between 7 and 12 were recruited at the Child Guidance Clinic, Institute of Mental Health, Singapore. The subjects with ADHD were diagnosed by child psychiatrists according to the DSM-IV (Gaub & Carlson, 1997). Additionally, parents were interviewed using the Diagnostic Interview Schedule for Children, which is based on the DSM-IV. 28 age and gender-matched healthy boys were recruited for the study. The controls had no current diagnosis or history of mental disorders. All the participants are right-handed. Written informed consent from the parents and assent forms from the child to partake in the studies and to allow imaging data to be used in further analyses were both obtained. Exclusion criteria for all subjects included history of epileptic seizures, mental retardation and an IQ of < 70 which was measured using Kaufman Brief Intelligence Test, Second Edition (Hays et al., 2002). Of these participants, 16 healthy subjects, 26 children with ADHD-C and 15 children with ADHD-I had available functional MRI data that passed quality control (see image preprocessing session for details). Prior to the study, two subjects with ADHD-C were on methylphenidate. They were only allowed to participate in study procedures after at least one month of washout. Demographic, imaging and clinical information of participants is shown in Table 1.

3. Behavioral assessments

The behavioral rating instrument for ADHD patients was the Child Behavior Checklist (CBCL) (Achenbach & Rescorla, 2001). The CBCL is a parent-rated questionnaire designed to obtain descriptions of a child's competencies and behavioral/emotional problems. It provides both empirical-based symptoms and dimensional constructs for psychopathology, and is well validated (Ferdinand, 2008). Allowing for the fact that ADHD often co-occurs with internalizing disorders as a few studies have reported (Chen et al., 2016), scores of CBCL sub-scales attention-deficit/hyperactivity problems and internalizing problems were derived as the primary outcome. The attention-deficit/hyperactivity problems scale sums scores for inattention and hyperactivity-impulsivity, which are the core symptoms in ADHD, and the internalizing problems scale comprises problems that are mainly within the self, reflecting anxiety disorder and social phobia of children. The mean and the standard deviation scores of the two scales of the participants are shown in Table 1. There was no difference in clinical symptoms between the drop-outs and the patients included in the analysis in ADHD group and ADHD subtype groups. There were no interactions between the ADHD groups and inclusion/exclusion groups (see Supplementary Table 1).

4. Image acquisition

All functional and structural images were collected at the Center for Cognitive Neuroscience, Duke-National University of Singapore Medical School using a 12-channel head coil on a 3-Tesla Tim Trio or a 20-channel head coil on a 3-Tesla Prisma scanner (Siemens, Germany) due to unavoidable system upgrade. The same imaging parameters were used for both scanners for maximum consistency. The RS-fMRI data using T2*-weighted echo planar images (repetition time = 2000 ms, echo time = 30 ms, flip angle = 90 degrees, field of view = 192 * 192 mm^2, voxel size = 3.0 mm isotropic, slice

Table 1
Subject demographic and behavioral characteristics.

		Healthy boys (N = 16)	ADHD (N = 41)		p-value
			ADHD-C (N = 26)	ADHD-I (N = 15)	
Age (years)		9.75 (1.73)	8.88 (1.47)		0.061
			8.88 (1.42)	8.87 (1.60)	0.175
Handedness (right: left)		15: 1	41: 0		0.106
			26: 0	15: 0	0.271
Ethnicity (Chinese: Indian)		16: 0	40: 1		0.529
			26: 0	14: 1	0.241
Max. absolute motion displacement (mm)		0.31 (0.47)	0.32 (0.36)		0.940
			0.37 (0.40)	0.22 (0.25)	0.505
Mean absolute motion displacement (mm)		0.09 (0.13)	0.08 (0.08)		0.776
			0.09 (0.09)	0.06 (0.05)	0.433
Number of volumes after motion scrubbing (modularity analysis)		204.31 (34.60)	191.02 (35.76)		0.209
			187.23 (34.55)	197.60 (38.07)	0.306
Children global assessment scale		–	57.20 (4.50)		–
			57.31 (3.76)	57.0 (5.78)	0.840
CBCL internalizing problems	Raw score	–	9.73 (6.78)		–
			11.44 (6.87)	6.87 (5.76)	0.037*
	T-score	–	57.98 (10.35)		–
			60.88 (8.80)	53.13 (11.20)	0.020*
CBCL attention deficit/hyperactivity Problems	Raw score	–	9.43 (2.44)		–
			10.24 (2.03)	8.07 (2.52)	0.005*
	T-score	–	67.28 (6.82)		–
			69.44 (5.85)	63.67 (6.97)	0.008*

Note: All participants are male. Continuous variables are expressed as mean (standard deviation). N: number of subjects. CBCL: Child Behavioral Checklist. One ADHD subject with combined subtype has missing clinical assessment scores. Maximal and mean absolute motion displacement are from the final 120 frames of each data set for the ICA analysis, while the number of volumes after motion scrubbing. * indicates significance of $p < .05$.

thickness = 3 mm, no gap, 36 axial slices, interleaved collection) were collected while the subjects were asked to relax and fixate on a cross centered on the screen. The RS-fMRI data collection (8 min 12 s altogether; 246 volumes) was broken up into two consecutive short runs to minimize motion artifacts; the duration for each of the two runs was 4 min 6 s each. The data of both runs were concatenated for further processing. An eye tracker was used to ensure that the children stayed awake for the entire RS-fMRI scan. The high-resolution structural T1-weighted magnetization prepared rapid gradient echo images (repetition time = 2300 ms, echo time = 2.98 ms, inversion time = 900 ms, flip angle = 90 degrees, field of view = 256 * 256 mm^2, voxel size = 1.0 mm isotropic) were collected for atlas registration of the RS-fMRI images. To minimize the influence of scanner difference, we included the scanner type as a covariate in all statistical analysis.

5. Image preprocessing

The resting-state fMRI images and structural MRI images were both preprocessed using a standard pipeline based on the FMRIB's Software Library (FSL, www.fmrib.ox.ac.uk/fsl) (Smith et al., 2004) and the Analysis of Functional NeuroImages software program (AFNI) (Cox, 1996) following our previous work (Wang et al., 2017). The structural image preprocessing included: 1) image noise reduction, 2) skull stripping, 3) linear and non-linear registration to the Montreal Neurological Institute (MNI) 152 standard space, and 4) segmentation of the brain into grey matter, white matter and cerebrospinal fluid (CSF) compartments. Preprocessing steps for the resting-state fMRI data included the following steps: The first five volumes of each data set were discarded to account for initial magnetic field instability when collecting those volumes. For ICA, preprocessing steps included interleaved slice-timing correction, motion correction using first functional image with skull, skull stripping, spatial smoothing using a 6 mm full width half maximum (FWHM) Gaussian kernel to improve signal-to-noise ratio and to reduce inter-subject variability, and grand mean scaling. Images were finally normalized to the Montreal Neurological Institute 152 stereotactic standard space of 2 mm isotropic resolution using a nonlinear registration tool (FNIRT). For modular structure analysis, the preprocessing steps included additional temporal band-pass filtering, detrending and nuisance signals reduction (details in Supplementary Materials).

Subsequently, considering that excessive motion may introduce spurious functional connectivity in brain networks (Power et al., 2012), motion scrubbing was performed on the preprocessed data. Framewise displacement and the rate of change of blood-oxygenation-level-dependent signal across the entire brain (DVARS) at each frame were calculated following a previous approach (Power et al., 2012) and frames with framewise displacement larger than 0.8 and DVARS larger than 0.05 were removed. For the subsequent group ICA, we kept 120 frames with lower framewise displacement values for each subject. For modularity analysis, the data after motion scrubbing (with varying length) were used, but the three groups did not differ in the number of volumes left (Table 1).

6. Within-network connectivity derivation

Group ICA was performed on the overall group preprocessed data (57 subjects) using Probabilistic Independent Component Analysis (Beckmann & Smith, 2004) with 25 components as implemented in MELODIC (Multivariate Exploratory Linear Decomposition into Independent Components) Version 3.14 in FSL. The generated independent components (ICs) were visually checked to identify those which best represent the large-scale group-level functional networks with reference to previous studies (Zhou et al., 2010; Beckmann et al., 2009).

To examine within-network differences in functional connectivity and extraction of individual IC time series for the following between-network analysis, the dual regression approach in FSL (Version 5.0.9) was applied to preprocessed images (Beckmann et al., 2009). After running a group-average ICA, dual regression estimated spatial maps for each subject. In its first stage, the group-spatial-maps were regressed into each subject's preprocessed 4D dataset to give a set of time courses. Those time courses were then regressed into the same 4D dataset to get a subject-specific set of spatial maps in the second stage.

7. Between-network connectivity calculation

For each subject, between-network connectivity for each pair of components of interest was obtained by the FSL Nets analysis package, which was implemented in Matlab2016a (http://fsl.fmrib.ox.ac.uk/fsl/fslwiki/FSLNets). The between-network connectivity was defined as the correlation between each pair of IC time courses of the participants, obtained from the earlier dual regression analysis. Comparisons of both full and partial correlations between each pair of components of interest were performed between groups. Partial correlation estimates only the direct connection strengths between pairs of networks, while full correlation allows for the influence of other network values on pairs of interest.

8. Modular community detection and modularity derivation

To characterize network modular structure, we derived the individual whole-brain functional connectivity matrix based on mean time series extracted from a set of 144 regions-of-interest (ROIs) defined by a previous data-driven functional parcellation scheme (Yeo et al., 2011). We chose this functional parcellation because it was derived from 1000 healthy subjects and it allows grouping of ROIs into 7 networks and subcortical regions for interpretation (Wang et al., 2017). Due to the lack of coverage in certain brain regions, 141 ROIs were used for network construction. At the individual level, we calculated the Pearson's correlations between the time-series of each pair of ROIs and then Fisher's r-to-z transformed them into the FC z-scores. To derive individual level network community structures, we used the Louvain method (Blondel et al., 2008; Jutla et al., 2011) followed by a consensus-based clustering method (Lancichinetti & Fortunato, 2012) with multiple resolution parameters γ (see Supplementary Methods). Resolution parameter γ determined the topological scale at which communities were detected. Large values of γ bias the algorithm toward detecting smaller communities. For each resolution parameter γ, we computed the modularity index (Blondel et al., 2008) of the network with final community structure for each participant, which quantified the strength of segregation into distinct networks. Higher values indicate stronger separation of networks.

8.1. Statistical analysis

Between-group differences in demographic properties and clinical assessments were tested respectively for 1) healthy controls and all subjects with ADHD, 2) healthy controls and subjects with ADHD combined subtype and 3) healthy controls and subjects with ADHD inattentive subtype. Either a two sample *t*-test, a one-way ANOVA (age, maximal and mean absolute motion displacement, CBCL subscale scores) or a chi-squared test (handedness, ethnicity and scanner type) was used.

To examine group differences in within-network connectivity, the spatial maps across groups of subjects was compared using randomise permutation testing in FSL (5000 permutations). The resulting group difference maps between groups for each component of interest were thresholded using threshold-free cluster enhancement with an alpha level of 0.05 (corrected at family-wise error (FWE) rate). Between-network FC and modularity index comparisons between groups were also conducted using randomise permutation testing in FSL (5000 permutations). An alpha level of 0.05 (FWE corrected) was applied when examining group differences in between-network FC and modularity index. The individual effects of age and scanner type were regressed out for all tests. To ensure that group differences in functional connectivity were not explained by differences in underlying grey matter volume, we later performed grey matter volume correction (details in Supplementary methods).

To examine whether there was a relationship between behavioral problems in children with ADHD and those within/between-network connections showing group differences, Pearson correlational analysis was performed to estimate the associations. Specifically, CBCL subscales Attention Deficit/Hyperactivity Problems and Internalizing Problems were used to represent clinical symptom severity. The individual effects of age and scanner type were first regressed out from the behavioral scores before the correlational analysis.

9. Results

There were no significant differences in the demographic variables (age, gender, handedness and ethnics) and imaging variables (maximal and mean absolute motion displacement, number of volumes, and scanner types) between the healthy control and ADHD or ADHD subtype groups (Table 1). Participants with ADHD-C displayed more severe CBCL attention deficit/hyperactivity problems and internalizing problems than participants with ADHD-I ($p = .005$ and .037 respectively).

9.1. Within-network connectivity: children with ADHD-C but not ADHD-I exhibited hyper-connectivity within the anterior DMN

25 ICs were produced from the group ICA on the dataset of 57 subjects. Of these 25 ICs, 8 were considered as noise or artifacts such as movement, white matter, or ventricles and were not subjected to further analysis. The resultant 17 ICs of interest (Fig. S1) were visually inspected with reference to previous studies and subjected to the subsequent dual regression analysis.

There were no significant within-network differences between children with ADHD and healthy controls. For the within-network comparison between ADHD subtypes and healthy controls, children with ADHD-C showed significant hyper-connectivity in the anterior DMN compared with healthy controls (FWE corrected $p < .05$, Fig. 1). No significant FC differences in any of the networks were observed between ADHD-I and healthy controls. For the within-network comparison between ADHD-I and ADHD-C, children with ADHD-C showed significant higher connectivity in the primary visual network than children with ADHD-I (FWE corrected $p < .05$, Fig. S2).

When we included grey matter volume of each network as covariates, all results remained with lower significance (see Supplementary Results).

9.2. Between-network connectivity: stronger connectivity between networks in ADHD group was driven by ADHD-C subtype

The between-network comparisons based on full correlations revealed that children with ADHD had significantly higher correlation between the left ECN and SN compared with age-matched healthy

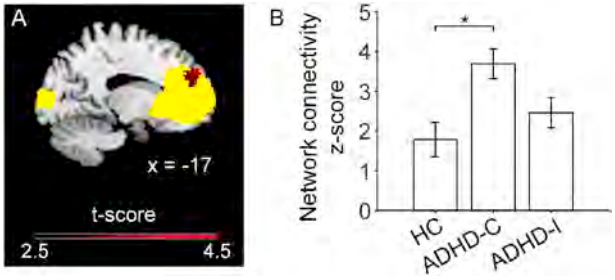

Fig. 1. Children with ADHD-C exhibited hyper-connectivity in the anterior default mode network (aDMN) compared to age-match healthy controls (HC). A. Brain slice highlighting the region showing greater functional connectivity (in red) within the anterior default network (in yellow) in ADHD-C group than HC group ($p < .05$ FWE corrected). In contrast, ADHD-I did not differ in intra-network connectivity from HC. B. The mean functional connectivity values across all voxels in the peak region highlighted in panel A was plotted for the three groups. Error bars indicate standard error. * represents FWE corrected $p < .05$.

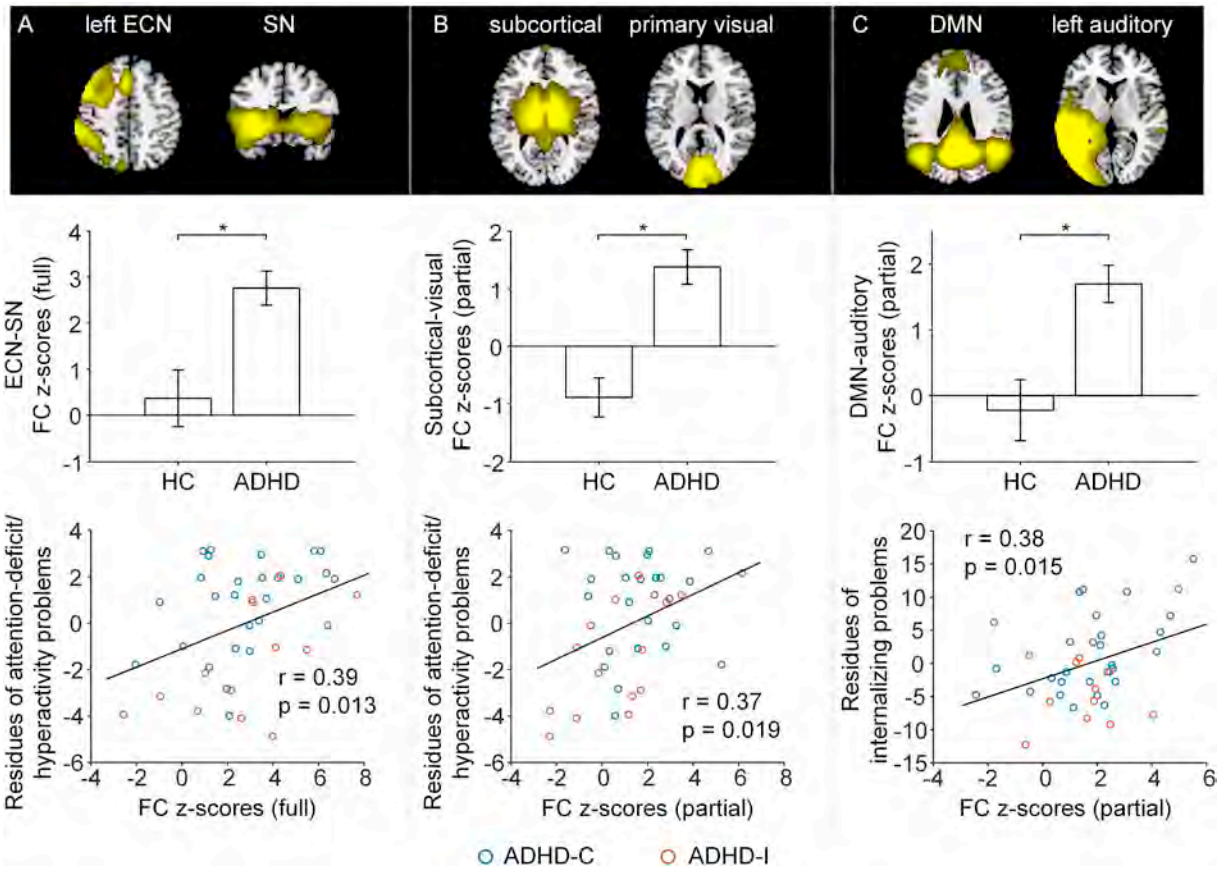

Fig. 2. Loss of between-network functional segregation in ADHD and its association with symptom severity. Row 1: Brain slices showing the spatial maps of the two network components. Row 2: Compared to controls, ADHD had higher functional connectivity between the left ECN and the salience network (full correlation, panel A), between subcortical and visual networks (partial correlation, panel B) and between the posterior DMN and left auditory network (partial correlation, panel C). The bars and error bars indicate mean and standard error respectively. * represents $p < .05$ FWE corrected for all the pairs between all the ICs of interest. Row 3: The loss of between network functional segregation related to symptom severity in ADHD participants including CBCL attention-deficit/hyperactivity problems (A & B) and CBCL internalizing problems (C) (red: ADHD inattentive subtype (ADHD-I); blue: ADHD combined subtype (ADHD-C)). Abbreviations: ECN: executive control network; SN: salience network; DMN: default mode network.

controls ($t = 3.883$, FWE corrected $p = .018$; Fig. 2A). For partial correlation networks, children with ADHD showed significantly higher correlation between the subcortical and the primary visual network ($t = 3.801$, FWE corrected $p = .025$; Fig. 2B) and significantly higher correlation between the posterior DMN and the left auditory network ($t = 3.596$, FWE corrected $p = .049$; Fig. 2C) compared with controls.

These observed between-network FC group differences between ADHD and controls were driven by participants with ADHD-C subtype, i.e., ADHD-C had stronger inter-network FC than healthy controls but ADHD-I did not. For full correlation networks, children with ADHD-C showed higher FC between the left ECN and the SN ($t = 3.549$, FWE corrected $p = .050$; Fig. 3A) and higher FC between the posterior DMN and the left auditory network ($t = 3.962$, FWE corrected $p = .016$; Fig. 3C) compared with controls. For partial correlation networks, children with ADHD-C showed higher FC between subcortical and the primary visual network ($t = 4.590$, FWE corrected $p = .002$; Fig. 3B) and higher FC between the posterior DMN and the left auditory network ($t = 3.571$, FWE corrected $p = .046$; Fig. 3D) compared with controls.

For the between-network comparison between ADHD-I and ADHD-C, children with ADHD-C showed significant higher connectivity (partial correlation) between the limbic and cerebellum network than children with ADHD-I ($t = 3.848$, FWE corrected $p = .026$; Fig. S2).

When grey matter volumes were included as covariates in statistical analysis, the results remained largely unchanged (see Supplementary Results).

9.3. Modularity: loss of modular segregation in ADHD group was driven by ADHD-C

Based on the community structure of whole-brain functional connectome, we found that children with ADHD showed reduced modularity compared to healthy controls (Fig. 4A; $p < .05$ for all values of γ). In line with the between-network results, the subtype analyses revealed significant reduction of modularity in children with ADHD-C (Fig. 4B; $p < .05$ for all values of γ), while children with ADHD-I showed no significant difference compared to healthy controls, with a mean modularity index falling between ADHD-C and healthy controls.

9.4. Abnormalities in network connectivity and modularity in ADHD related to symptoms severity

Greater FC between the left ECN and the SN (full correlation, $r = 0.39$, $p = .013$) and greater FC between subcortical and the visual network (partial correlation, $r = 0.37$, $p = .019$) were associated with more severe attention deficit/hyperactivity problems across ADHD participants (Fig. 2A & B). The FC (partial correlation) between the posterior DMN and the left auditory network positively related to internalizing problems across all ADHD patients ($r = 0.38$, $p = .015$; Fig. 2C). Reduced network modularity was associated with more internalizing problems across all ADHD patients (Fig. 4C, Supplementary Results). Similar trend was also observed within each sub-group (see Supplementary Results).

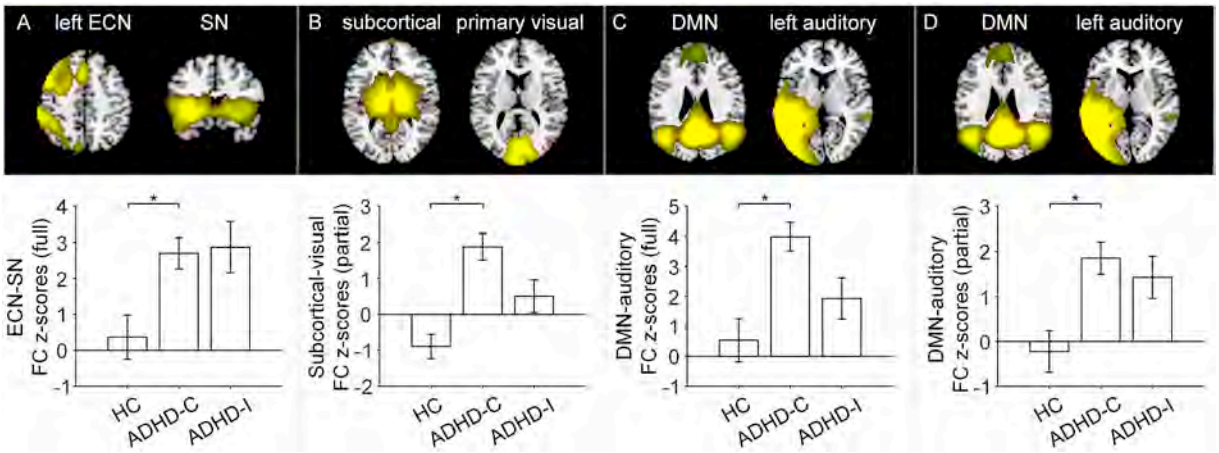

Fig. 3. Differential degree of between-network hyper-connectivity in ADHD combined (ADHD-C) and inattentive (ADHD-I) subtypes. Row 1: Brain slices showing the spatial maps of the two network components. Row 2: Compared to controls, ADHD-C had higher functional connectivity between left ECN and the salience network (full correlation, panel A), between subcortical and visual network (partial correlation, panel B) and between posterior DMN and left auditory network (full correlation, panel C; partial correlation, panel D). The bars and error bars indicate mean and standard error respectively. * represents $p < .05$ FWE corrected for all the pairs between all the ICs of interest.

10. Discussion

In the current study, we demonstrate atypical patterns of whole-brain large-scale network connectivity in childhood ADHD and its subtypes. Within networks, we observed hyper-connectivity within the anterior DMN only in children with ADHD-C but not in children with ADHD-I, when compared with healthy controls. Children with ADHD had higher correlation between the left ECN and SN, subcortical and visual networks, and posterior DMN and left auditory network compared to healthy controls. Subsequent analyses revealed that these differences were mainly driven by the atypical between-network connectivity in the ADHD-C subtype. Consistently, graph theoretical analysis revealed lower modularity in ADHD-C but not ADHD-I compared with controls, indicating weaker network segregation in ADHD-C. Importantly, these abnormal between-network connectivity and modularity metrics were associated with symptom severity in ADHD children. These findings suggest that different network topology phenotypes underly the neurobiological heterogeneity of ADHD subtypes.

10.1. Loss of brain network segregation underlies the lag of maturation in childhood ADHD

Both longitudinal and cross-sectional multimodal neuroimaging studies have convincingly reported maturational lags in ADHD (Bos et al., 2017; Sripada et al., 2014; Shaw et al., 2007; Janssen et al., 2017; Castellanos & Aoki, 2016). Specifically, Bos and colleagues showed increased FC in medial prefrontal cortex (mPFC) within the DMN in children with ADHD and a negative relation between the FC in the mPFC and age both in typically developing children and children with ADHD, reflecting reduced or delayed functional segregation of prefrontal brain regions (Bos et al., 2017). Besides increased FC in medial prefrontal cortex revealed in children with ADHD-C, between-network differences between healthy children and children with ADHD were observed in the current study, and were not explained by intra-subject variance of grey matter volumes. The observed increased FC between the SN and the ECN in childhood ADHD might implicate an interrupted balance of salience-network-induced coordination (Castellanos & Proal, 2012). The SN is involved in monitoring for behaviorally relevant salient stimuli and in interrupting ongoing activity when appropriate, playing a dynamic switching role between the DMN and the ECN, which respectively support self-related (or internally directed) and goal-oriented (or externally directed) cognition, to guide appropriate responses to salient stimuli (Uddin, 2015). The inappropriate engagement of the SN with the ECN in ADHD children underlie interrupted salience processing of internal and external stimuli which dominates attention capturing.

The increased between-network FC as well as the decreased network modularity in childhood ADHD might implicate a delay in

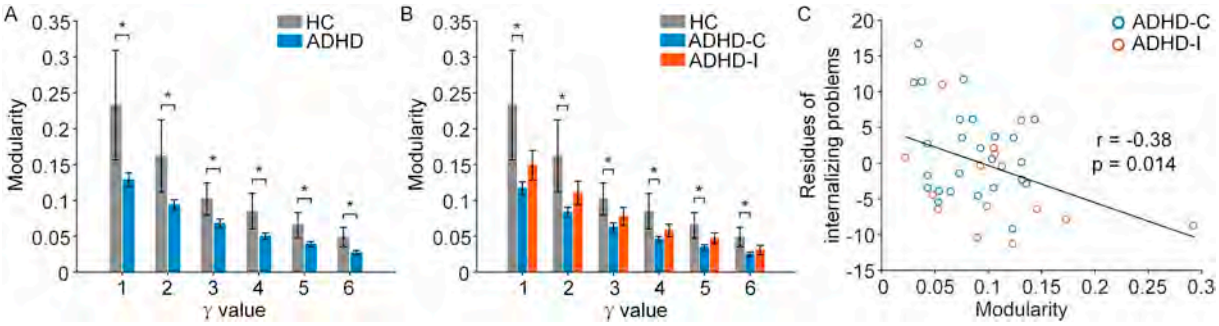

Fig. 4. Children with ADHD showed lower brain network modularity compared to healthy controls (HCs). (A) ADHD group had lower network modularity scores. The horizontal axis represents a range of γ values (i.e., multiple resolution levels) for the community partition algorithm. Data were reported as mean values and standard errors (* indicates $p < .05$, $p = .033, .039, .042, .031, .031, .030$ for $\gamma = 1$ to 6 respectively). (B) Children with ADHD combined subtype (ADHD-C) but not children with ADHD inattentive subtype (ADHD-I) had reduced modularity compared with controls (* indicates $p < .05$, $p = .019, .021, .025, .019, .015, .021$ for $\gamma = 1$ to 6 respectively). C. Lower modularity scores were associated with more CBCL internalizing problems in subjects with ADHD across almost all γ values ($\gamma = 2$ presented here as an example).

development. It has been proposed that ADHD involves a lag in brain maturation in terms of both the brain's developing functional architecture as well as its structural features such as grey matter volume or cortical thickness (Cao et al., 2014a; Betzel et al., 2014; Sripada et al., 2014). The human brain functional network operates as a hierarchical, modular structure, subdividing the network into groups of nodes, with the maximum possible number of within-group links, and the minimal possible number of between-group links. This functional segregation among intrinsic connectivity networks will increase with age along the developmental trajectory from childhood to adolescence (Baum et al., 2017; Barber et al., 2015). However, compared with healthy controls, children with ADHD exhibited a loss of functional segregation between certain core brain systems. As can be seen in Fig. 2, subcortical and visual networks, as well as DMN and auditory network, were anti-correlated in healthy children, while in children with ADHD they were positively correlated. Consistent with this finding, compared with controls, children with ADHD exhibit significantly reduced modularity of the final robust community structure, across multiple topological scales of community detection. To a certain degree, this atypical integration in childhood ADHD might be due to a lag of maturation in childhood ADHD.

Such loss of network segregation and modularity nicely mirrors previous findings of hyper-connectivity in ADHD. For example, emotion dysregulation in ADHD individuals may arise from deficits in orienting toward, recognizing, and/or allocating attention to emotional stimuli, which implicate dysfunction within a striato-amygdalo-prefrontal cortical network (Shaw et al., 2014). Hulvershorn et al. showed that higher emotional dysregulation was associated with hyper-connectivity between amygdala and anterior cingulate cortex at rest in youth with ADHD aged 6–13 years old (Hulvershorn et al., 2014). Similarly, adolescents with ADHD had higher amygdala activation and hyper-connectivity between amygdala and lateral prefrontal cortex compared to controls during fearful face processing (Posner et al., 2011). Notably, the observed abnormal between-network connectivity (i.e., hyper-connectivity between cortical and subcortical networks) and modularity here were significantly correlated with attention-deficit/hyperactivity problems or internalizing problems in ADHD children (Fig. 2), indicating that the large-scale brain functional network topology disruptions could potentially reflect behavioral phenotype and severity in ADHD.

10.2. Brain network topology phenotype underlie childhood ADHD heterogeneity

The current study highlights the distinction between the ADHD combined subtype and ADHD inattentive subtype in children, providing a biological basis for exploring symptom dimensions and revealing potential targets for precision treatments. ADHD is increasingly understood as a disorder of specific brain networks, with emphasis often placed on the DMN, which has been implicated in ADHD-related behaviors including mind-wandering and attentional fluctuations, and in its interactions with other networks hypothesized to underlie attentional dysfunctions (Barber et al., 2015; Kucyi et al., 2015; Posner et al., 2014; Fair et al., 2010). However, most previous studies did not distinguish the ADHD subtypes and differentiate children and adolescents. Evidence suggests that the developmental trajectory of functional connectivity in children to adults would spread variably (Nomi & Uddin, 2015). The current study included age-matched subtypes and healthy controls, which demonstrated hyper-connectivity within the anterior DMN only in childhood ADHD-C compared with healthy controls. This suggests that the ADHD-C subtype has more localized connectivity within medial prefrontal cortex, which may underlie abnormal function of filtering relevant signals.

The observed abnormalities of between-network connectivity were also exhibited in participants with ADHD-C but not in participants with ADHD-I compared with healthy children. Similarly, ADHD-C but not ADHD-I showed significantly lower modularity compared with controls. In contrast, FC and modularity bars of ADHD-I fell in between those of healthy controls and ADHD-C, which might potentially reflect the different behavior phenotypes of the two subtypes. Taken together, these findings suggest that the clinical distinction between the inattentive and combined subtypes of ADHD may be reflected in differential aberrations of the underlying brain functional organization. These neuroimaging-based brain network topological measures help to shed lights on detailed brain-behavior phenotype associations in neuropsychiatric disorders (Barber et al., 2015; Nielson et al., 2017).

10.3. Limitations and future directions

The current study employed a cross-sectional design with a moderate sample size. When considering development of brain network topology as a continuum ranging from “local to distributed” organization (Fair et al., 2009), our findings suggested that children with ADHD may lack behind their typically developing peers, i.e., with decreased functional network segregation compared with age-matched healthy controls. However, this hypothesis remains to be tested in a longitudinal design to distinguish between delayed and altered maturation of neural networks. Future longitudinal studies on larger samples could provide additional insight on the differential or similar longitudinal trajectories of brain functional networks in ADHD subtypes. Moreover, brain structural connectivity analysis is needed to examine structure-function relationships related to ADHD heterogeneity; comprehensive symptoms assessments are needed to examine specific brain circuits underlying behavioral phenotype of ADHD. In addition, although one month wash-out period was given to all ADHD patients to minimize medication effects, there might still be some long lasting residual effects (e.g., two patients with methylphenidate) (Schrantee et al., 2016). Lastly, this study involved the use of two scanner types due to unavoidable system upgrade, which might introduce systematic signal differences. However, we kept all imaging parameters the same and there were no systematic differences in scanner types between groups. We have also taken into account scanner type in all statistical analysis to mitigate such concern.

Taken together, this study provides a comprehensive understanding of the whole-brain intrinsic network connectivity of childhood ADHD, suggesting that the loss of functional segregation might underlie the delayed or altered brain maturation trajectory in childhood ADHD. The large-scale brain functional network topology phenotype might provide the neurobiological basis underlying childhood ADHD heterogeneity. Further development with machine learning methods in larger sample may help individual stratification and treatment planning in ADHD.

Acknowledgement

We would like to thank all subjects for their participation in this study. This work was supported by the National Medical Research Council, Singapore (NMRC/NIG11may025 to CGL and NMRC/CIRG/1390/2014 to JZ), and Duke-NUS Medical School Signature Research Program funded by Ministry of Health, Singapore.

Conflict of interest

The authors report no biomedical financial interests or potential conflicts of interest.

Appendix A. Supplementary data

Supplementary data to this article can be found online at https://doi.org/10.1016/j.nicl.2018.11.010.

References

Achenbach, T.M., Rescorla, L., 2001. ASEBA School-Age Forms & Profiles. Aseba Burlington, VT.

Barber, A.D., Jacobson, L.A., Wexler, J.L., Nebel, M.B., Caffo, B.S., Pekar, J.J., et al., 2015. Connectivity supporting attention in children with attention deficit hyperactivity disorder. Neuroimage Clin. 7, 68–81.

Baum, G.L., Ciric, R., Roalf, D.R., Betzel, R.F., Moore, T.M., Shinohara, R.T., et al., 2017 Jun 05. Modular segregation of structural brain networks supports the development of executive function in youth. Curr. Biol. 27 (11), 1561–1572 (e8).

Beckmann, C.F., Smith, S.M., 2004. Probabilistic independent component analysis for functional magnetic resonance imaging. IEEE Trans. Med. Imaging 23 (2), 137–152.

Beckmann, C.F., Mackay, C.E., Filippini, N., Smith, S.M., 2009. Group comparison of resting-state FMRI data using multi-subject ICA and dual regression. NeuroImage 47 (Suppl. 1), S148.

Bertolero, M.A., Yeo, B.T., D'Esposito, M., 2015. The modular and integrative functional architecture of the human brain. Proc. Natl. Acad. Sci. 112 (49) (E6798-E807).

Betzel, R.F., Byrge, L., He, Y., Goñi, J., Zuo, X.-N., Sporns, O., 2014. Changes in structural and functional connectivity among resting-state networks across the human lifespan. NeuroImage 102, 345–357.

Biswal, B., Zerrin Yetkin, F., Haughton, V.M., Hyde, J.S., 1995. Functional connectivity in the motor cortex of resting human brain using echo-planar mri. Magn. Reson. Med. 34 (4), 537–541.

Blondel, V., Guillaume, J., Lambiotte, R., Lefebvre, E., 2008. Fast Unfolding of Community Hierarchies in large network. J. Stat. Mech. 1008.

Bos, D.J., Oranje, B., Achterberg, M., Vlaskamp, C., Ambrosino, S., Reus, M.A., et al., 2017. Structural and functional connectivity in children and adolescents with and without attention deficit/hyperactivity disorder. J. Child Psychol. Psychiatry 58 (7), 810–818.

Cao, M., Wang, J.-H., Dai, Z.-J., Cao, X.-Y., Jiang, L.-L., Fan, F.-M., et al., 2014a. Topological organization of the human brain functional connectome across the lifespan. Develop. Cognit. Neurosci. 7, 76–93.

Cao, M., Shu, N., Cao, Q., Wang, Y., He, Y., 2014 Decb. Imaging functional and structural brain connectomics in attention-deficit/hyperactivity disorder. Mol. Neurobiol. 50 (3), 1111–1123.

Castellanos, F.X., Aoki, Y., 2016. Intrinsic functional connectivity in attention-deficit/hyperactivity disorder: a science in development. Biol. Psych.: Cognitive Neurosci. Neuroimag 1 (3), 253–261.

Castellanos, F.X., Proal, E., 2012 Jan. Large-scale brain systems in ADHD: beyond the prefrontal-striatal model. Trends Cogn. Sci. 16 (1), 17–26.

Chen, T.J., Ji, C.Y., Wang, S.S., Lichtenstein, P., Larsson, H., Chang, Z., 2016. Genetic and environmental influences on the relationship between ADHD symptoms and internalizing problems: a Chinese twin study. Am. J. Med. Genet. B Neuropsychiatr. Genet. 171 (7), 931–937.

Cox, R.W., 1996. AFNI: software for analysis and visualization of functional magnetic resonance neuroimages. Comput. Biomed. Res. 29 (3), 162–173.

dos Santos, Siqueira A., Biazoli Junior, C.E., Comfort, W.E., Rohde, L.A., Sato, J.R., 2014. Abnormal functional resting-state networks in ADHD: graph theory and pattern recognition analysis of fMRI data. Biomed. Res. Int. 2014, 380531.

Fair, D.A., Cohen, A.L., Power, J.D., Dosenbach, N.U., Church, J.A., Miezin, F.M., et al., 2009. Functional brain networks develop from a “local to distributed” organization. PLoS Comput. Biol. 5 (5), e1000381.

Fair, D.A., Posner, J., Nagel, B.J., Bathula, D., Dias, T.G., Mills, K.L., et al., 2010 Dec 15. Atypical default network connectivity in youth with attention-deficit/hyperactivity disorder. Biol. Psychiatry 68 (12), 1084–1091.

Fair, D., Nigg, J.T., Iyer, S., Bathula, D., Mills, K.L., Dosenbach, N.U., et al., 2013. Distinct neural signatures detected for ADHD subtypes after controlling for micro-movements in resting state functional connectivity MRI data. Front. Syst. Neurosci. 6, 80.

Ferdinand, R.F., 2008. Validity of the CBCL/YSR DSM-IV scales anxiety problems and affective problems. J. Anxiety Disord. 22 (1), 126–134.

Fox, M.D., Raichle, M.E., 2007 Sep. Spontaneous fluctuations in brain activity observed with functional magnetic resonance imaging. Nat. Rev. Neurosci. 8 (9), 700–711.

Francx, W., Oldehinkel, M., Oosterlaan, J., Heslenfeld, D., Hartman, C.A., Hoekstra, P.J., et al., 2015. The executive control network and symptomatic improvement in attention-deficit/hyperactivity disorder. Cortex 73, 62–72.

Gaub, M., Carlson, C.L., 1997. Behavioral characteristics of DSM-IV ADHD subtypes in a school-based population. J. Abnorm. Child Psychol. 25 (2), 103–111.

Haack, L.M., Villodas, M., McBurnett, K., Hinshaw, S., Pfiffner, L.J., 2017. Parenting as a mechanism of change in psychosocial treatment for youth with ADHD, predominantly inattentive presentation. J. Abnorm. Child Psychol. 45 (5), 841–855.

Hays, J.R., Reas, D.L., Shaw, J.B., 2002. Concurrent validity of the Wechsler abbreviated scale of intelligence and the Kaufman brief intelligence test among psychiatric inpatients. Psychol. Rep. 90 (2), 355–359.

Hulvershorn, L.A., Mennes, M., Castellanos, F.X., Di Martino, A., Milham, M.P., Hummer, T.A., et al., 2014. Abnormal amygdala functional connectivity associated with emotional lability in children with attention-deficit/hyperactivity disorder. J. Am. Acad. Child Adolesc. Psychiatry 53 (3), 351–361 e1.

Janssen, T., Hillebrand, A., Gouw, A., Geladé, K., Van Mourik, R., Maras, A., et al., 2017. Neural network topology in ADHD; evidence for maturational delay and default-mode network alterations. Clin. Neurophysiol. 128 (11), 2258–2267.

Jutla IS, Jeub LG, Mucha PJ. A generalized Louvain method for community detection implemented in MATLAB. URL http://netwiki amath unc edu/GenLouvain. 2011.

Kessler, R.C., Adler, L.A., Barkley, R., Biederman, J., Conners, C.K., Faraone, S.V., et al., 2005 Jun 01. Patterns and predictors of attention-deficit/hyperactivity disorder persistence into adulthood: results from the national comorbidity survey replication. Biol. Psychiatry 57 (11), 1442–1451.

Khundrakpam, B.S., Lewis, J.D., Zhao, L., Chouinard-Decorte, F., Evans, A.C., 2016. Brain connectivity in normally developing children and adolescents. NeuroImage 134, 192–203.

Khundrakpam, B.S., Lewis, J.D., Reid, A., Karama, S., Zhao, L., Chouinard-Decorte, F., et al., 2017. Imaging structural covariance in the development of intelligence. NeuroImage 144, 227–240.

Kucyi, A., Hove, M.J., Biederman, J., Van Dijk, K.R., Valera, E.M., 2015 Sep. Disrupted functional connectivity of cerebellar default network areas in attention-deficit/hyperactivity disorder. Hum. Brain Mapp. 36 (9), 3373–3386.

Lancichinetti, A., Fortunato, S., 2012. Consensus clustering in complex networks. Sci. Rep. 2, 336.

Lei, D., Ma, J., Du, X., Shen, G., Jin, X., Gong, Q., 2014. Microstructural abnormalities in the combined and inattentive subtypes of attention deficit hyperactivity disorder: a diffusion tensor imaging study. Sci. Rep. 4, 6875.

Menon, V., 2013. Developmental pathways to functional brain networks: emerging principles. Trends Cogn. Sci. 17 (12), 627–640.

Meunier, D., Lambiotte, R., Fornito, A., Ersche, K., Bullmore, E.T., 2009. Hierarchical modularity in human brain functional networks. Front. Neuroinform. 3, 37.

Nielson, J.L., Cooper, S.R., Yue, J.K., Sorani, M.D., Inoue, T., Yuh, E.L., et al., 2017. Uncovering precision phenotype-biomarker associations in traumatic brain injury using topological data analysis. PLoS One 12 (3), e0169490.

Nomi, J.S., Uddin, L.Q., 2015. Developmental changes in large-scale network connectivity in autism. Neuroimage Clin. 7, 732–741.

Posner, J., Nagel, B.J., Maia, T.V., Mechling, A., Oh, M., Wang, Z., et al., 2011. Abnormal amygdalar activation and connectivity in adolescents with attention-deficit/hyperactivity disorder. J. Am. Academy Child Adolescent Psych. 50 (8), 828–837 e3.

Posner, J., Park, C., Wang, Z., 2014 Mar. Connecting the dots: a review of resting connectivity MRI studies in attention-deficit/hyperactivity disorder. Neuropsychol. Rev. 24 (1), 3–15.

Power, J.D., Fair, D.A., Schlaggar, B.L., Petersen, S.E., 2010. The development of human functional brain networks. Neuron 67 (5), 735–748.

Power, J.D., Barnes, K.A., Snyder, A.Z., Schlaggar, B.L., Petersen, S.E., 2012. Spurious but systematic correlations in functional connectivity MRI networks arise from subject motion. NeuroImage 59 (3), 2142–2154.

Saad, J.F., Griffiths, K.R., Kohn, M.R., Clarke, S., Williams, L.M., Korgaonkar, M.S., 2017. Regional brain network organization distinguishes the combined and inattentive subtypes of attention deficit hyperactivity disorder. Neuroimage Clin. 15, 383–390.

Sahakian, B.J., Bruhl, A.B., Cook, J., Killikelly, C., Savulich, G., Piercy, T., et al., 2015 Sep 19. The impact of neuroscience on society: cognitive enhancement in neuropsychiatric disorders and in healthy people. Philos. Trans. R. Soc. Lond. Ser. B Biol. Sci. 370 (1677), 20140214.

Sanefuji, M., Craig, M., Parlatini, V., Mehta, M.A., Murphy, D.G., Catani, M., et al., 2017. Double-dissociation between the mechanism leading to impulsivity and inattention in attention deficit hyperactivity disorder: a resting-state functional connectivity study. Cortex 86, 290–302.

Schrantee, A., Tamminga, H.G., Bouziane, C., Bottelier, M.A., Bron, E.E., Mutsaerts, H.-J.M., et al., 2016. Age-dependent effects of methylphenidate on the human dopaminergic system in young vs adult patients with attention-deficit/hyperactivity disorder: a randomized clinical trial. JAMA Psych. 73 (9), 955–962.

Seymour, K.E., Miller, L., 2017. ADHD and depression: the role of poor frustration tolerance. Current Develop. Disorders Rep. 4 (1), 14–18.

Shang, C.-Y., Sheng, C., Yang, L.-K., Chou, T.-L., Gau, S.S.-F., 2017. Differential brain activations in adult attention-deficit/hyperactivity disorder subtypes: a counting Stroop functional MRI study. Brain Imaging Behav. 1–9.

Sharma, A., Couture, J., 2014 Feb. A review of the pathophysiology, etiology, and treatment of attention-deficit hyperactivity disorder (ADHD). Ann. Pharmacother. 48 (2), 209–225.

Shaw, P., Eckstrand, K., Sharp, W., Blumenthal, J., Lerch, J., Greenstein, D., et al., 2007. Attention-deficit/hyperactivity disorder is characterized by a delay in cortical maturation. Proc. Natl. Acad. Sci. 104 (49), 19649–19654.

Shaw, P., Stringaris, A., Nigg, J., Leibenluft, E., 2014. Emotion dysregulation in attention deficit hyperactivity disorder. Am. J. Psychiatr. 171 (3), 276–293.

Sidlauskaite, J., Sonuga-Barke, E., Roeyers, H., Wiersema, J.R., 2016. Altered intrinsic organisation of brain networks implicated in attentional processes in adult attention-deficit/hyperactivity disorder: a resting-state study of attention, default mode and salience network connectivity. Eur. Arch. Psychiatry Clin. Neurosci. 266 (4), 349–357.

Smith, S.M., Jenkinson, M., Woolrich, M.W., Beckmann, C.F., Behrens, T.E., Johansen-Berg, H., et al., 2004. Advances in functional and structural MR image analysis and implementation as FSL. NeuroImage 23 (S208-S19).

Sripada, C.S., Kessler, D., Angstadt, M., 2014 Sep 30. Lag in maturation of the brain's intrinsic functional architecture in attention-deficit/hyperactivity disorder. Proc. Natl. Acad. Sci. U. S. A. 111 (39), 14259–14264.

Uddin, L.Q., 2015 Jan. Salience processing and insular cortical function and dysfunction. Nat. Rev. Neurosci. 16 (1), 55–61.

Wang, C., Lee, J., Ho, N.F., Lim, J.K., Poh, J.S., Rekhi, G., et al., 2017. Large-scale network topology reveals heterogeneity in individuals with at risk mental state for psychosis: findings from the longitudinal youth-at-risk study. Cereb. Cortex 1–10.

Yeo, B.T., Krienen, F.M., Sepulcre, J., Sabuncu, M.R., Lashkari, D., Hollinshead, M., et al., 2011 Sep. The organization of the human cerebral cortex estimated by intrinsic functional connectivity. J. Neurophysiol. 106 (3), 1125–1165.

Zhao, Q., Li, H., Yu, X., Huang, F., Wang, Y., Liu, L., et al., 2017. Abnormal resting-state functional connectivity of insular subregions and disrupted correlation with working memory in adults with attention deficit/hyperactivity disorder. Front. Psychiatry 8, 200.

Zhou, J., Greicius, M.D., Gennatas, E.D., Growdon, M.E., Jang, J.Y., Rabinovici, G.D., et al., 2010. Divergent network connectivity changes in behavioural variant frontotemporal dementia and Alzheimer's disease. Brain 133 (5), 1352–1367.